Polymer 50 (2009) 4363–4371

Contents lists available at ScienceDirect

Polymer

journal homepage: www.elsevier.com/locate/polymer

Catalytic activity of a thermosensitive hydrophilic diblock copolymer-supported 4-*N*,*N*-dialkylaminopyridine in hydrolysis of *p*-nitrophenyl acetate in aqueous buffers

Thomas G. O'Lenick, Xiaoming Jiang, Bin Zhao*

Department of Chemistry, University of Tennessee, 567 Buehler Hall, Knoxville, TN 37996, USA

ARTICLE INFO

Article history:
Received 31 May 2009
Received in revised form
28 June 2009
Accepted 4 July 2009
Available online 9 July 2009

Keywords:
Thermosensitive polymers
Block copolymer micelles
Catalysis

ABSTRACT

This article reports on the synthesis of a thermosensitive hydrophilic diblock copolymer with the thermosensitive block containing a catalytic 4-*N*,*N*-dialkylaminopyridine and the study of the effect of thermo-induced micellization on its catalytic activity in the hydrolysis of *p*-nitrophenyl acetate (NPA). The block copolymer, poly(ethylene oxide)-*b*-poly(methoxydi(ethylene glycol) methacrylate-*co*-2-(*N*-methyl-*N*-(4-pyridyl)amino)ethyl methacrylate), was synthesized by ATRP. The critical micellization temperatures (CMTs) of this block copolymer in the pH 7.06 and 7.56 buffers were 40 and 37 °C, respectively. The polymer was used as the catalyst for the hydrolysis of NPA. We found that below CMT, the logarithm of initial hydrolysis rate changed linearly with inverse temperature. With the increase of temperature above CMT, the plot of logarithm of reaction rate versus $1/T$ leveled off, i.e., the hydrolysis rate did not increase as much as anticipated from the Arrhenius equation. This is likely because the reaction rate at temperatures above CMT was controlled by mass transport of NPA from bulk water phase to the core of micelles where the catalytic sites were located.

1. Introduction

Polymer-supported organic catalysts have been a subject of intensive research in the past decades [1–3]. In addition to offering the advantages of facile recovery and reuse of the catalysts, polymers create a distinct microenvironment, which can be tailored by varying polymer structures, allowing the tuning of catalytic activities of supported catalysts and the control of the compatibility between different types of catalytic groups [1–22]. Of great interest are stimuli-responsive polymer catalysts, which exhibit tunable or switchable catalytic activities in response to environmental stimuli [23–25]. These catalysts are highly desired for many applications as the reaction rates can be conveniently controlled by environmental stimuli. Up to date, there are only a few examples of such polymer organocatalysts in the literature. Tanaka and coworkers reported an imidazole-containing polymer gel consisting of *N*-isopropylacrylamide (NIPAm), 4(5)-vinylimidazole, and a crosslinker [23]. The gel can undergo reversible swelling and shrinking in response to the composition changes of the mixed solvent of water and methanol. They observed that when the gel collapsed, the catalytic activity for esterolysis was dramatically enhanced, which was believed to result from the increased affinity of the substrate to the collapsed hydrophobic network. Khokhlov et al. synthesized thermosensitive random copolymers of 1-vinylimidazole and *N*-vinylcaprolactam or NIPAm, and found that above the lower critical solution temperatures (LCSTs) of the copolymers, the hydrolysis rates of an activated ester were higher than predicted from the Arrhenius equation, presumably because both the substrate and the catalytic imidazole units were enriched at the interface of polymer aggregates [24]. The observed effect was larger for the copolymer of NIPAm and 1-vinylimidazole than for the copolymer of *N*-vinylcaprolactam and 1-vinylimidazole. With further increasing temperature, the aggregates became unstable and the activities decreased appreciably.

Compared with thermosensitive catalyst-containing random copolymers, which form unstable large aggregates at temperatures above the LCSTs, block copolymers are more advantageous for developing polymer catalysts with tunable or switchable activities as they can self-assemble into well-defined stable micelles upon application of external stimuli. Patrickios et al. synthesized poly(2-(*N*,*N*-dimethylamino)ethyl methacrylate)-*b*-poly(2-(1-imidazolyl)-ethyl methacrylate) (PDMAEMA-*b*-PImEMA) by group transfer polymerization [26–28]. Different from their original speculation that the micellization of block copolymers with PImEMA forming the core would accelerate the reaction, they did not observe

* Corresponding author. Tel.: +1 865 974 3399; fax: +1 865 974 3454.
E-mail address: zhao@ion.chem.utk.edu (B. Zhao).

0032-3861/$ – see front matter © 2009 Elsevier Ltd. All rights reserved.
doi:10.1016/j.polymer.2009.07.007

enhanced catalytic activities of the block copolymers compared with the random copolymers, likely because the hydrophobicity of short PImEMA blocks was not sufficient for extensive micellization. Using reversible addition–fragmentation chain transfer polymerization, Liu et al. synthesized doubly hydrophilic thermosensitive diblock copolymers, PNIPAm-*b*-poly(*N*-vinylimidazole), which self-assembled into micelles with the PNIPAm block forming the core and the catalytic block forming the corona at elevated temperatures [25]. They found that the esterolysis rates were enhanced pronouncedly at temperatures above the critical micellization temperatures (CMTs).

Despite these efforts, the issue, how the micellization affects the catalytic activity of a stimulus-responsive block copolymer with an organic catalyst being incorporated into the core-forming block, has not been elucidated. Understanding this issue will enable a rational design of stimuli-responsive polymeric catalysts. One can envision that if the partition coefficient of the substrate between micelles and bulk water phase is sufficiently high, it could be concentrated in the core of micelles, resulting in a higher reaction rate. On the other hand, the formation of micelles with the catalyst buried inside the core could impose a mass transport limitation, which might suppress the reaction rate. In the present work, we synthesized a thermosensitive hydrophilic diblock copolymer with the thermosensitive block containing catalytic 4-*N*,*N*-dialkylaminopyridine (DAAP) units and studied the effect of thermo-induced micellization of the block copolymer on the hydrolysis rate of *p*-nitrophenyl acetate (NPA), an activated ester, in aqueous buffers. DAAPs are highly efficient nucleophilic catalysts for many organic reactions, including acylation of sterically hindered alcohols, hydrolysis of activated esters, and Baylis–Hillman reaction [6–22,29–32]. Scheme 1 illustrates the synthesis of block copolymer poly(ethylene oxide)-*b*-poly(methoxydi(ethylene glycol) methacrylate-*co*-2-(*N*-methyl-*N*-(4-pyridyl)amino)ethyl methacrylate) PEO-*b*-P(DEGMMA-*co*-MAPMA) from a PEO macroinitiator by atom transfer radical polymerization (ATRP). PDEGMMA is a thermosensitive water-soluble polymer with a LCST of 25 °C in water; it belongs to a new family of thermosensitive hydrophilic polymers that contain a short oligo(ethylene glycol) pendant in each monomer unit [33–42]. The thermo-induced micellization of the block copolymer in aqueous buffers (Scheme 2) was studied by dynamic light scattering. The block copolymer was then used as catalyst for the hydrolysis of NPA at various temperatures from below to above the CMT and the hydrolysis rates of NPA were measured by UV–vis spectrometry.

2. Experimental section

2.1. Materials

Methoxydi(ethylene glycol) methacrylate (DEGMMA, or di(ethylene glycol) methyl ether methacrylate, 95%, Aldrich) was dried with calcium hydride, distilled under a reduced pressure, and stored in a refrigerator prior to use. CuCl (99.995%, Aldrich) was purified according to the procedure described in the literature [43–45] and stored in a desiccator. $CuCl_2$ (anhydrous, 99%), *p*-nitrophenyl acetate (NPA, 97%), acetonitrile (99.5%), *N*,*N*-dimethylformamide (extra dry, with molecular sieves), and sodium tetraborate decahydrate were purchased from Acros and used as-received. Potassium dihydrogen phosphate (≥99%) and 1,1,4,7,10,10-hexamethyltriethylenetetramine (97%) were obtained from Aldrich–Sigma and used as-received. Ethyl 2-bromoisobutyrate (98%, Aldrich) was dried over calcium hydride, distilled under a reduced pressure, and stored in a desiccator prior to use. The synthesis and characterization of 4-(*N*-methyl-*N*-(2-hydroxyethyl)amino)pyridine, 2-(*N*-methyl-*N*-(4-pyridyl)amino)-ethyl methacrylate (MAPMA), and macroinitiator PEO-Br (PEO with molecular weight of 5000 Da and one end functionalized with an ATRP initiator) can be found in previous publications [32,46,47].

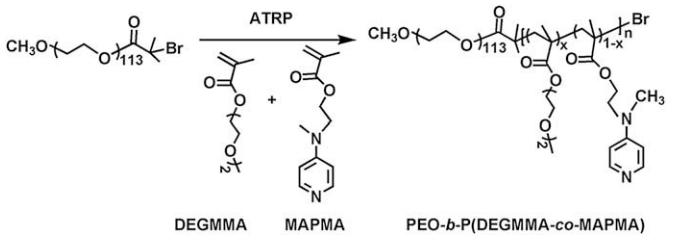

Scheme 1. Synthesis of thermosensitive block copolymer PEO-*b*-P(DEGMMA-*co*-MAPMA) with the thermosensitive block containing a catalytic 4-*N*,*N*-dialkylaminopyridine by atom transfer radical polymerization.

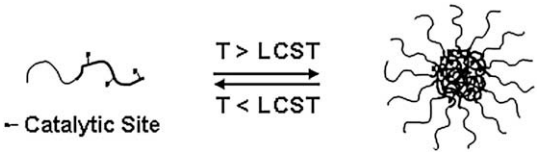

Scheme 2. Thermo-induced micellization of PEO-*b*-P(DEGMMA-*co*-MAPMA) in an aqueous buffer.

2.2. Characterization

Size exclusion chromatography (SEC) was carried out at ambient temperature using PL-GPC 50 Plus (an integrated GPC/SEC system from Polymer Laboratories, Inc) with a differential refractive index detector, one PSS GRAL guard column (50 × 8 mm, 10 μm particles, Polymer Standards Service-USA, Inc.), and two PSS GRAL linear columns (each 300 × 8 mm, 10 μm, molecular weight range from 500 to 1,000,000 according to Polymer Standards Service-USA, Inc.). The data were processed using Cirrus™ GPC/SEC software (Polymer Laboratories, Inc.). *N*,*N*-Dimethylformamide (DMF) was used as the carrier solvent at a flow rate of 1.0 mL/min. Standard monodisperse polystyrenes (Polymer Laboratories, Inc.) were used for calibration. ^{1}H NMR (300 MHz) spectra were recorded on a Varian Mercury 300 NMR spectrometer and the residual solvent proton signal was used as the internal standard.

The cloud points of poly(methoxydi(ethylene glycol) methacrylate-*co*-2-(*N*-methyl-*N*-(4-pyridyl)amino)ethyl methacrylate) (P(DEGMMA-*co*-MAPMA)) in 10 mM aqueous phosphate buffers with pH of 7.06 and 7.56 at a concentration of 0.020 wt% were measured by turbidimetry. The optical transmittances of polymer solutions at various temperatures were recorded at wavelength of 500 nm with a UV–vis spectrometer (Biomate 5 from Thermospectronic, Inc.). The sample cell was thermostated with an external water bath of a Fisher Scientific Isotemp refrigerated circulator. At each temperature, the solutions were equilibrated for 5 min.

2.3. Synthesis of PEO-b-P(DEGMMA-co-MAPMA)

Copper (I) chloride (4.9 mg, 4.9×10^{-5} mol), copper (II) chloride (2.9 mg, 2.2×10^{-5} mol), macroinitiator PEO-Br (223.6 mg, 4.34×10^{-5} mol), DEGMMA (1.005 g, 5.34 mmol), MAPMA (82.7 mg of a 53.0 wt% solution of MAPMA in DMF, 43.8 mg MAPMA, 1.99×10^{-4} mol), and DMF (1.004 g) were added into a two-necked flask. The reaction mixture was stirred under a dry nitrogen atmosphere. 1,1,4,7,10,10-Hexamethyltriethylenetetramine (HMTETA, 16.2 mg, 7.03×10^{-5} mol) was injected via a microsyringe; the

solution turned light green immediately. After the reaction mixture was degassed by three freeze–pump–thaw cycles, the flask was placed in a 75 °C oil bath. The polymerization was stopped after 156 min by removing the flask from the oil bath and opening it to air. The mixture was diluted with THF and passed through a short neutral aluminum oxide/silica gel column to remove the copper catalyst. The polymer was precipitated in hexanes three times from its THF solution. The polymer was then dissolved in THF and the solution was stored in a refrigerator (temperature: ~4 °C). The precipitate was removed by filtration. The solution was then concentrated and precipitated in a mixture of hexanes/diethyl ether (v/v: 50/50). After being dried in high vacuum, the block copolymer was obtained as a very viscous liquid (0.696 g). SEC analysis results (polystyrene standards): $M_{n,SEC} = 26\,600$ Da, polydispersity index (PDI) = 1.12. The numbers of DEGMMA and MAPMA units in the block copolymer were calculated from the ^{1}H NMR spectrum using the integral values of the peak at 8.2 ppm ($N(CHCH)_2$ of MAPMA units), the peaks from 3.9 to 4.5 ppm (CH_2OCO of DEGMMA and MAPMA units), and the peaks from 3.0 to 3.9 ppm (OCH_2 from the PEO block and DEGMMA units plus CH_2OCH_3 of DEGMMA units and the C–N(CH_3)CH_2 of MAPMA units). The numbers of DEGMMA (n_{DEGMMA}) and MAPMA units (n_{MAPMA}) in the block copolymer were 117 and 3, respectively. A random copolymer P(DEGMMA-*co*-MAPMA) was prepared by ATRP using ethyl 2-bromoisobutyrate as initiator under the same conditions for the synthesis of PEO-*b*-P(DEGMMA-*co*-MAPMA). $M_{n,SEC} = 19100$ Da, PDI = 1.11, $n_{DEGMMA} = 92$ and $n_{MAPMA} = 3$.

2.4. Determination of pK_a of the MAPMA units in PEO-*b*-P(DEGMMA-*co*-MAPMA)

A series of 10 mM aqueous buffer solutions were made by dissolving sodium tetraborate decahydrate (borax) or potassium dihydrogen phosphate in deionized water. The pH values of buffer solutions were adjusted by the addition of a 1.0 M NaOH or a 1.0 M HCl solution and measured by a pH meter. To determine the pK_a of the MAPMA units in PEO-*b*-P(DEGMMA-*co*-MAPMA) at room temperature, the UV–vis spectra of the block copolymer in these buffer solutions were recorded at room temperature with a UV–vis spectrometer (Biomate 5 from Thermospectronic, Inc.). A typical UV–vis experiment is described below. A phosphate buffer (pH = 7.14, 1.069 g) was added into a quartz cuvette, followed by the injection of an aqueous polymer solution (24.8 mg, 0.95 wt%) via a microsyringe. The solution was then agitated with a glass pipette. The cuvette was placed into the cell holder of the instrument and the UV–vis spectrum of the block copolymer was recorded. DAAPs are known to exhibit a 20 nm shift in λ_{max} when the basic (B, nonprotonated) and conjugated acid forms (BH^+, protonated) are compared. The absorbances at 280 nm (from protonated MAPMA, BH^+) and 260 nm (from nonprotonated MAPMA, B) were used for the calculation of pK_a [9]. The absorbances of PEO-*b*-P(DEGMMA-*co*-MAPMA) at pH = 1 and 13 were measured from 0.1 N aqueous HCl and 0.1 N NaOH solutions, respectively. A similar procedure was used to measure the pK_a of MAPMA units in PEO-*b*-P(DEGMMA-*co*-MAPMA) at 44 °C.

2.5. Dynamic light scattering study of thermo-induced micellization of PEO-*b*-P(DEGMMA-*co*-MAPMA) in aqueous buffer solutions

The thermo-induced micellization of PEO-*b*-P(DEGMMA-*co*-MAPMA) in aqueous buffers was studied by dynamic light scattering (DLS). The block copolymer PEO-*b*-P(DEGMMA-*co*-MAPMA) was dried in high vacuum for >3 h. Aqueous solutions of PEO-*b*-P(DEGMMA-*co*-MAPMA) with a concentration of 0.020 wt% were prepared by use of 10 mM phosphate buffers with pH of 7.06 and 7.56. The polymer solutions were sonicated in an ultrasonic ice/water bath for 5 min to ensure complete dissolution. Note that in the hydrolysis experiments, a solution of NPA in acetonitrile was injected into the polymer solution via a microsyringe; the concentration of acetonitrile in the final solution was 1.6 wt%. Considering that the LCST transition of the thermosensitive block of PEO-*b*-P(DEGMMA-*co*-MAPMA) could be affected by the presence of a small amount of acetonitrile, we injected a calculated amount of acetonitrile into the polymer solutions for DLS study to ensure that the concentration of acetonitrile was the same as that in the hydrolysis experiments.

DLS measurements were conducted with a Brookhaven Instruments BI-200SM goniometer equipped with a PCI BI-9000AT digital correlator, a temperature controller, and a solid-state laser (model 25-LHP-928-249, $\lambda = 633$ nm) at a scattering angle of 90°. The polymer solutions, containing 1.6 wt% acetonitrile, were filtered into borosilicate glass tubes with an inner diameter of 7.5 mm by the use of 0.2 μm filters. The glass tubes were then sealed with a PE stopper. The solutions were gradually heated from room temperature to 50 °C. At each temperature, the solutions were equilibrated for 30 min prior to data recording. The time correlation functions were analyzed with a Laplace inversion program (CONTIN).

2.6. Kinetics studies of the hydrolysis of *p*-nitrophenyl acetate in aqueous buffers using PEO-*b*-P(DEGMMA-*co*-MAPMA) as catalyst

The hydrolysis reactions of NPA were performed in 10 mM aqueous phosphate buffer solutions with pH of 7.06 and 7.56. The buffers were made by dissolving KH_2PO_4 in deionized water and the pH values were adjusted by addition of an aqueous NaOH solution and measured with a pH meter (Accumet AB 15 pH meter from Fisher Scientific, calibrated with pH = 4.01, 7.00, and 10.01 standard buffer solutions).

The kinetics studies of the hydrolysis of NPA were conducted in a quartz cuvette using a Hewlett Packard 8542A Diode Array UV–vis spectrophotometer equipped with a Hewlett Packard 89090A Peltier temperature controller. In all hydrolysis experiments, the concentrations of NPA and the MAPMA units of the block copolymer in the reaction medium were 2.9×10^{-4} M and 2.2×10^{-5} M, respectively. The absorbance of the ionized form of the hydrolysis product *p*-nitrophenol at 400 nm was recorded as a function of time by a computer program. A typical procedure for the NPA hydrolysis experiment is described below. A 0.020 wt% solution of PEO-*b*-P(DEGMMA-*co*-MAPMA) in a 10 mM phosphate buffer with pH of 7.06 (1.100 g) was added into a quartz cuvette equipped with a small magnetic stir bar. The cuvette was then placed into the cell holder of the UV–vis spectrometer with a preset temperature. After the solution was equilibrated for 25 min, a background scan was performed to record the absorbance of the polymer solution. A solution of NPA in acetonitrile (17.5 mg, 0.34 wt%) was injected into the cuvette via a microsyringe and the reaction mixture was immediately agitated with a glass pipette for 5 s. The UV–vis spectra of the reaction mixture were recorded as a function of time by a computer program. The time at which the NPA solution was injected was taken as $t = 0$ s. The absorbance at 400 nm was plotted versus time and the initial slope was obtained by linear regression of the first five points. The initial rates of the hydrolysis of NPA were calculated by using equation (1) [24,32].

$$V = \frac{dA_{400}}{dt}\frac{1}{\varepsilon b}\frac{1}{f} \quad (1)$$

where dA_{400}/dt is the initial slope of the variation of the absorbance at 400 nm (A_{400}) with time, ε is the extinction coefficient of ionized *p*-nitrophenol, b is the optical path length (1 cm), and f is the fraction of ionized *p*-nitrophenol in the buffer used in the

hydrolysis experiment. The product of extinction coefficient ε and fraction of ionized *p*-nitrophenol *f* is equal to the apparent coefficient ε' of *p*-nitrophenol in a buffer with a specific pH, which can be obtained by using the concentration of *p*-nitrophenol instead of the concentration of ionized *p*-nitrophenol in the calculations. The apparent extinction coefficients ε' ($=\varepsilon f$) of *p*-nitrophenol in the pH 7.06 and 7.56 buffers were 9446 and 12025 L mol^{-1} cm^{-1}, respectively, obtained by a method described below. A series of solutions of *p*-nitrophenol with different concentrations were made by the use of a buffer with pH of either 7.06 or 7.56, and their absorbances at 400 nm were recorded with a UV–vis spectrometer. The apparent extinction coefficient was obtained by linear regression of the plot of the absorbance at 400 nm versus nominal concentration of *p*-nitrophenol.

3. Results and discussion

3.1. Synthesis of thermosensitive hydrophilic block copolymer PEO-b-P(DEGMMA-co-MAPMA) with the thermosensitive block containing a DAAP catalyst

This work is intended to study the effect of thermo-induced micellization of a hydrophilic block copolymer in aqueous buffers on the catalytic activity of a DAAP catalyst that is incorporated into the thermosensitive block. DAAPs are highly efficient nucleophilic catalysts widely used in many organic reactions including hydrolysis of activated esters [6–22,29–32]. We chose the hydrolysis of *p*-nitrophenyl acetate, an activated ester, in aqueous buffers for studying the catalytic activity of a thermosensitive block copolymer-supported DAAP catalyst because this reaction proceeds cleanly to yield *p*-nitrophenol via a known pathway (Scheme 3) and the reaction can be conveniently followed by UV–vis spectrometry due to the absorbance of ionized *p*-nitrophenol at 400 nm [9,24,32].

The thermosensitive hydrophilic block copolymer, PEO-*b*-P(DEGMMA-*co*-MAPMA), was synthesized from macroinitiator PEO-Br by ATRP of a mixture of DEGMMA and MAPMA with a molar ratio of 100:3.7 at 75 °C using CuCl/$CuCl_2$/HMTETA as catalytic system in DMF. We used a small amount of MAPMA in the copolymerization for two reasons: (i) it is known that DAAPs are superior nucleophilic organocatalysts for the hydrolysis of *p*-nitrophenyl esters [6–9]; (ii) the incorporation of a small amount of MAPMA into the thermosensitive block will not change the thermosensitive property too much [32]. Size exclusion chromatography analysis of the purified block copolymer showed a monomodal peak with a number average molecular weight $M_{n,SEC}$ of 26 600 Da (relative to polystyrene standards) and a polydispersity index of 1.12 (Fig. 1a). On the basis of the degree of polymerization of the PEO block (DP of PEO block = 113), the numbers of DEGMMA and MAPMA units in the thermosensitive block were calculated from the ^{1}H NMR spectrum (Fig. 1b) and they were 117 and 3, respectively. The molar ratio of DEGMMA to MAPMA units in the block copolymer (100:2.6) is close to the feed ratio in the polymerization mixture (100:3.7). For comparison of thermoresponsive properties, a random copolymer of DEGMMA and MAPMA, P(DEGMMA-*co*-MAPMA), was synthesized by ATRP using a small molecule initiator, ethyl 2-bromoisobutyrate, under the same conditions for the synthesis of the block copolymer. The $M_{n,SEC}$ determined by SEC using polystyrene calibration is 19 100 Da and the PDI is 1.11. The numbers of DEGMMA and MAPMA units in the random copolymer are 92 and 3, respectively.

3.2. pK_a of the MAPMA units in block copolymer PEO-b-P(DEGMMA-co-MAPMA)

The hydrolysis rate of an activated ester in an aqueous solution with a DAAP as catalyst is heavily dependent on the concentration of nonprotonated DAAP, which is in turn dependent on the solution pH [6–9,32]. Thus, it is necessary to study its pK_a. The pK_a value of the MAPMA units in PEO-*b*-P(DEGMMA-*co*-MAPMA) was determined spectrophotometrically following a method described in the literature [9]. DAAPs are known to exhibit a 20 nm shift in λ_{max} when the basic (B, nonporotonated) and conjugated acid forms (BH^+, protonated) are compared, the peaks appearing typically at 260 and 280 nm, respectively [6–9,32]. The following equation was used to calculate the molar fraction of nonprotonated DAAP units, $x(B)$, at pH = *p* [9]:

$$x(B) = \frac{[A_{280}/A_{260}]_{pH1} - [A_{280}/A_{260}]_{pHp}}{[A_{280}/A_{260}]_{pH1} - [A_{280}/A_{260}]_{pH13}} \quad (2)$$

where A_{280} and A_{260} are the absorbances at 280 and 260 nm, respectively. The absorbances at pH = 1 and 13 were obtained from the UV–vis spectra of the block copolymer in a 0.1 N aqueous HCl solution and a 0.1 N NaOH solution, respectively. A series of aqueous buffers with salt concentrations of 10 mM and various pH values were prepared and used to make solutions of PEO-*b*-P(DEGMMA-*co*-MAPMA) for UV–vis measurements. The ratio of [B]/[BH^+] at each pH was calculated, and the pK_a value was then determined by the use of Henderson–Hasselbalch equation:

$$pH = pK_a + n\log([B]/[BH^+]) \quad (3)$$

where *n* is a measure of deviation from ideal titration behavior [9,32].

Fig. 2 shows the plot of log([B]/[BH^+]) versus pH for PEO-*b*-P(DEGMMA-*co*-MAPMA) in aqueous buffers at room temperature. The pK_a of the MAPMA units in the block copolymer, obtained by linear regression ($R = 0.999$, $n = 1.29$, Fig. 2), was 7.91. We previously reported that the pK_a of small molecule 4-(*N*-methyl-*N*-(2-hydroxyethyl)amino)pyridine (EGMAP) was 9.31 [32]. Note that EGMAP is the precursor for the synthesis of monomer MAPMA. Thus, the pK_a value of the MAPMA units in the block copolymer is 1.40 pH units lower than that of EGMAP, indicating that the incorporation of a DAAP into a polymer has a significant effect on its pK_a value. This observation is consistent with our previous result

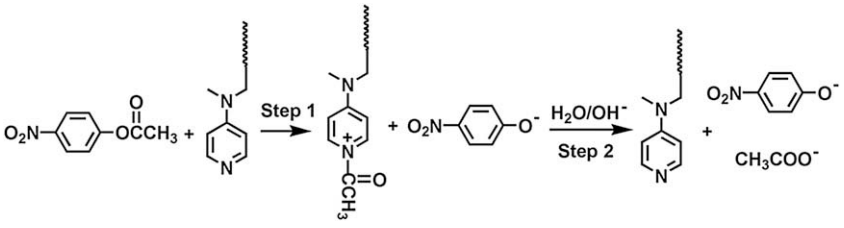

Scheme 3. Hydrolysis of *p*-nitrophenyl acetate catalyzed by a *N*,*N*-dialkylaminopyridine.

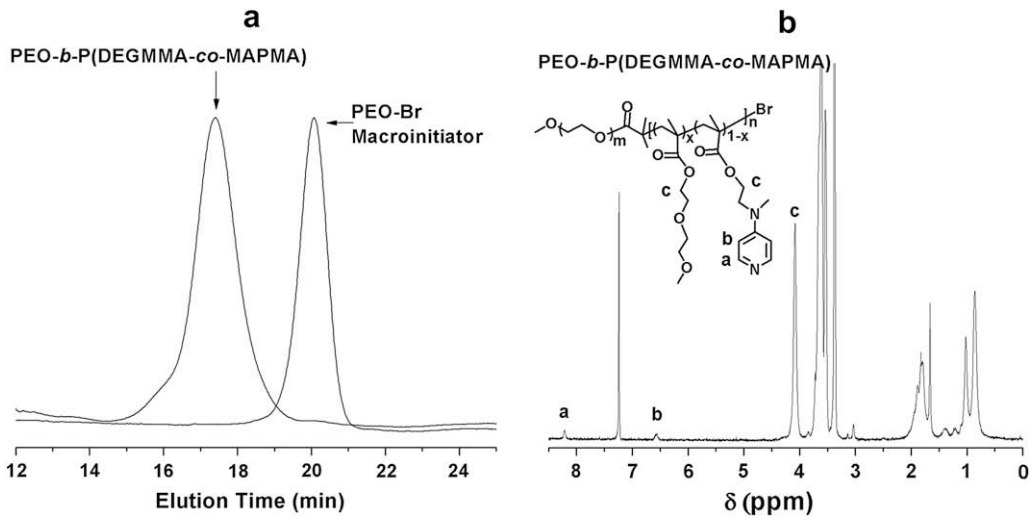

Fig. 1. (a) Size exclusion chromatography analysis of macroinitiator PEO-Br and the block copolymer PEO-*b*-P(DEGMMA-*co*-MAPMA), and (b) ^{1}H NMR spectrum of PEO-*b*-P(DEGMMA-*co*-MAPMA) in $CDCl_3$.

and those reported in the literature for the polymer-supported DAAPs [6–9,32]. Since the molar content of MAPMA units in the thermosensitive block was very small, only 2.5% (approximately one MAPMA unit every 40 monomer units in the P(DEGMMA-*co*-MAPMA) block), the electrostatic repulsive interaction among protonated DAAP units, which has been used to explain the lower pK_a values of polymer-supported DAAPs [8], is unlikely the predominant cause of the decreased pK_a value of PEO-*b*-P(DEGMMA-*co*-MAPMA). We believe that the main reason, as discussed by Urry [48], is that the introduction of charges (protonation of DAAP) onto a thermosensitive water-soluble polymer chain disrupts the "ordered" water structures around the hydrophobic moieties of the thermosensitive block and the charges on the MAPMA units compete with the hydrophobic groups for water molecules for hydration. Thus, to achieve the same degree of protonation of MAPMA units on a thermosensitive polymer chain, a lower solution pH, compared with small molecule EGMAP, is required. Since the nonprotonated DAAP is the actual nucleophilic catalyst, a lower pK_a makes the polymer catalyst more attractive than small molecule DAAPs because the reaction can be carried out at a milder pH at a reaction rate that can only be obtained at a higher pH with a small molecule DAAP as catalyst. For the same reason, we chose phosphate buffers with pH of 7.06 and 7.56, which are close to the pK_a of PEO-*b*-P(DEGMMA-*co*-MAPMA), as reaction media for the hydrolysis of NPA with the block copolymer as catalysts.

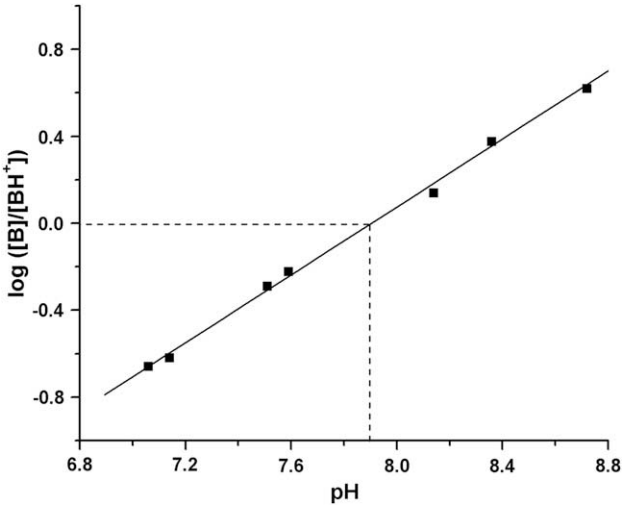

Fig. 2. Plot of log([B]/[BH$^+$]) versus pH for the MAPMA units in the block copolymer PEO-*b*-P(DEGMMA-*co*-MAPMA) in aqueous buffers with various pH values at room temperature, where [B] and [BH$^+$] are the concentrations of nonprotonated and protonated MAPMA units, respectively.

3.3. Cloud points of random copolymer P(DEGMMA-co-MAPMA) in aqueous phosphate buffers with pH of 7.06 and 7.56

We first studied the thermosensitive property of a random copolymer of DEGMMA and MAPMA with a similar molar ratio as in the block copolymer. The cloud points (CPs) of P(DEGMMA-*co*-MAPMA) in aqueous phosphate buffers with pH of 7.06 and 7.56 were determined by turbidimetry. Fig. 3 shows the optical transmittances of 0.020 wt% solutions of P(DEGMMA-*co*-MAPMA) in the two buffers at wavelength of 500 nm as a function of temperature in both heating and cooling processes. The optical transmittance began to decrease at 30 °C for the pH 7.56 polymer solution and 32.5 °C for the pH 7.06 solution upon increasing temperature. If 50% of the transmittance change is used for the determination of CP, the CP of the random copolymer was 34 °C in the pH 7.06 buffer and 31 °C in the pH 7.56 aqueous buffer. The cloud point of P(DEGMMA-*co*-MAPMA) in the pH 7.06 buffer is 3 °C higher than that at pH = 7.56. This is reasonable because at pH = 7.06 more MAPMA units are protonated, making the polymer more hydrophilic, and thus the coil-to-globule transition occurs at a higher temperature. From Fig. 3, one can also find that for both solutions there was essentially no hysteresis between the heating and cooling processes. The thermo-induced LCST transitions of this random copolymer in the two buffers were reversible.

3.4. Thermo-induced micellization of PEO-b-P(DEGMMA-co-MAPMA) in aqueous buffer solutions with pH of 7.06 and 7.56

Dynamic light scattering was employed to study the thermo-induced micellization of PEO-*b*-P(DEGMMA-*co*-MAPMA) in 10 mM phosphate buffers with pH of 7.06 and 7.56, the solutions used as reaction media for the hydrolysis of NPA. The block copolymer concentration in both buffers was 0.020 wt%, same as that in the

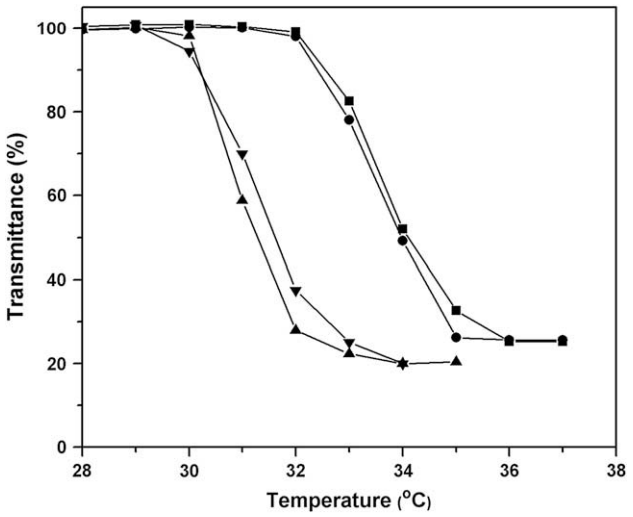

Fig. 3. Optical transmittance of 0.020 wt% solutions of P(DEGMMA-*co*-MAPMA) in 10 mM phosphate buffers with pH of 7.56 (▲ heating and ▼ cooling) and 7.06 (● heating and ■ cooling) as a function of temperature. The transmittances were recorded at wavelength of 500 nm with a UV–vis spectrometer.

hydrolysis experiments. It should be noted that in the hydrolysis experiments, NPA was added in the form of its solution in acetonitrile; the final solution contained 1.6 wt% acetonitrile. Since the presence of a small amount of acetonitrile could affect the thermoresponsive properties of the thermosensitive block and thus the CMT of the block copolymer in the aqueous buffers, we added a predetermined amount of acetonitrile into the polymer solutions for the DLS experiments such that the acetonitrile concentration was the same as that in the hydrolysis experiments.

Fig. 4 shows the results from a DLS study of a 0.020 wt% solution of PEO-*b*-P(DEGMMA-*co*-MAPMA) in the pH 7.06 phosphate buffer. When the temperature was below 39 °C, the scattering intensity was very low and the hydrodynamic size of the block copolymer was small, <8 nm, suggesting that the block copolymer was molecularly dissolved in the aqueous buffer solution. When the temperature reached 40 °C, the scattering intensity began to increase and the hydrodynamic size jumped to ~80 nm, indicating that the thermosensitive block was undergoing a temperature-induced hydration–dehydration transition. With further increasing the temperature to 41 °C and beyond, the value of D_h became stabilized around 43 nm. The CMT determined from the plot of scattering intensity versus temperature in the heating process is 40 °C (Fig. 4a). The data from the cooling process essentially superimposed the heating curve. When the temperature was decreased to 39 °C, the block copolymer micelles dissociated into the unimers.

Fig. 5 shows the data from a DLS study of a 0.020 wt% solution of PEO-*b*-P(DEGMMA-*co*-MAPMA) in the pH 7.56 buffer. Similar to the observations for the pH 7.06 buffer, the block copolymer self-assembled into micelles with an apparent hydrodynamic diameter of ~43 nm when the temperature was higher than 40 °C. This thermo-induced micellization was reversible. Decreasing the temperature caused the micelles to dissociate into the unimers (Fig. 5). The CMT, determined from the heating curve in Fig. 5a was 37 °C, which is 3 °C lower than that in the pH 7.06 buffer, consistent with our observations of the cloud points of random copolymer P(DEGMMA-*co*-MAPMA) in the two buffers. At a lower pH, more MAPMA monomer units were protonated, rendering the thermosensitive block more hydrophilic and thus a higher LCST transition temperature. Calculations show that 82% of MAPMA units were protonated at pH = 7.06, while 65% MAPMA units were protonated in the pH 7.56 buffer. Note that the CMT of PEO-*b*-P(DEGMMA-*co*-MAPMA) in each buffer was 6 °C higher than the CP of the corresponding random copolymer solution. This is consistent with our previous observations [46,47]. It is known that the LCST transition temperature is slightly higher when a thermosensitive polymer is attached to a hydrophilic block [49–51].

3.5. Hydrolysis of *p*-nitrophenyl acetate with PEO-b-P(DEGMMA-*co*-MAPMA) as catalyst in the pH 7.06 and 7.56 buffer solutions at various temperatures

The hydrolysis reactions of *p*-nitrophenyl acetate with PEO-*b*-P(DEGMMA-*co*-MAPMA) as catalyst were carried out in 10 mM aqueous phosphate buffers with pH of 7.06 and 7.56 under the stirring condition in the temperature range of 30–48 °C. The reactions were monitored by recording the absorbance at 400 nm (A_{400nm}) as a function of time by a UV–vis spectrometer via a computer program. For all hydrolysis experiments, $[NPA] = 2.9 \times 10^{-4}$ M and $[MAPMA] = 2.2 \times 10^{-5}$ M. Fig. 6 shows A_{400nm} as a function of time for the hydrolysis of NPA in the pH 7.56 buffer at (a) 30 °C, which was below the CMT, and (b) 44 °C, which was above the CMT. Clearly, the absorbance A_{400nm} increased smoothly and, in the beginning, linearly with the increase of time at both temperatures. The initial hydrolysis rate was derived by a linear regression of the first five points and the use of equation (1)

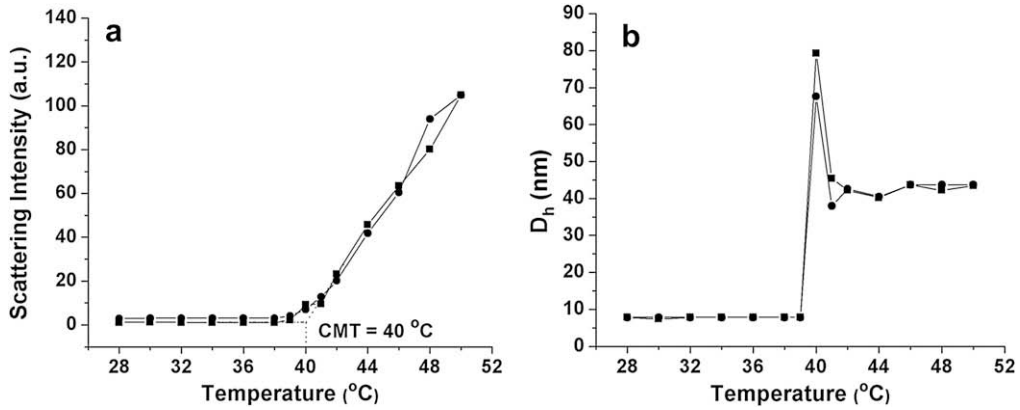

Fig. 4. (a) Scattering intensity at the scattering angle of 90° and (b) apparent hydrodynamic diameter, D_h, as a function of temperature, obtained from a dynamic light scattering study of a 0.020 wt% solution of PEO-*b*-P(DEGMMA-*co*-MAPMA) in the pH = 7.06 aqueous phosphate buffer (■ heating; ● cooling).

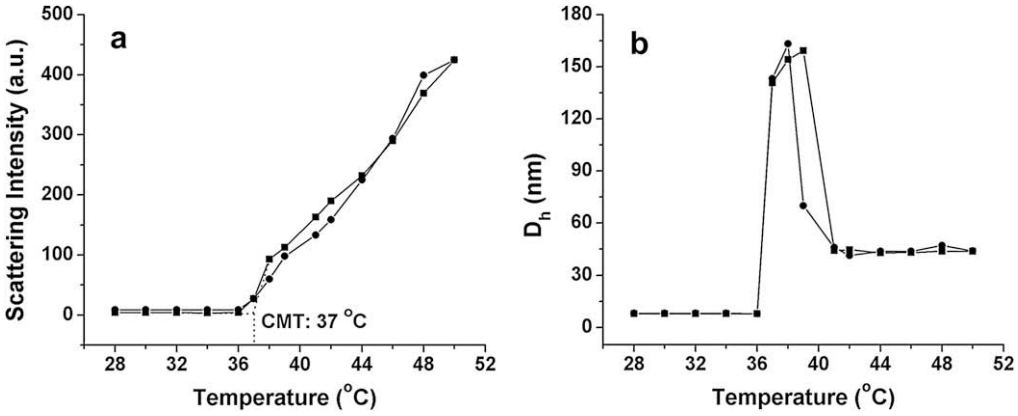

Fig. 5. (a) Scattering intensity at the scattering angle of 90° and (b) apparent hydrodynamic diameter, D_h, as a function of temperature, obtained from a dynamic light scattering study of a 0.020 wt% solution of PEO-*b*-P(DEGMMA-*co*-MAPMA) in a pH = 7.56 aqueous buffer solution (■ heating; ● cooling).

as described in the Experimental section. Since the buffer might also contribute to the initial rate of the hydrolysis of NPA, we also measured the background rates by performing the reactions at the same conditions except without addition of any DAAP catalyst. We found that the background rate accounted for a small fraction of the total rate, e.g., 5.3% of the total rate catalyzed by the block copolymer in the pH 7.56 buffer at 30 °C and 16.5% at 48 °C. To better understand the catalytic activity of the block copolymer-supported DAAP catalyst before and after the thermo-induced micellization, we derived the net initial rates of the hydrolysis of NPA by subtracting the corresponding background rates from the overall rates for all temperatures.

The effect of temperature on reaction rate constant is usually expressed by Arrhenius equation, that is, ln k changes linearly with inverse temperature $1/T$ [24,25,32]. Fig. 7 shows the plots of logarithm of net initial rate (log V) versus $1/T$ for the hydrolysis of NPA using PEO-*b*-P(DEGMMA-*co*-MAPMA) as catalyst. A linear relationship between log V and $1/T$ was observed in the range of 30–38 °C for the reactions in the pH 7.56 buffer and 30–40 °C for the reactions in the pH 7.06 buffer, indicating that the hydrolysis of NPA with PEO-*b*-P(DEGMMA-*co*-MAPMA) as catalyst in these temperature ranges followed the Arrhenius behavior. The two curves in these ranges were essentially in parallel. From DLS studies, the CMT of PEO-*b*-P(DEGMMA-*co*-MAPMA) was 37 °C in the pH 7.56 buffer and 40 °C in the pH 7.06 buffer. Thus, the block copolymer was in the unimer state at these temperatures except 38 °C in the pH 7.56 buffer.

From Fig. 7, one can also find that the reaction at any temperature in the pH = 7.56 buffer was consistently faster than that at pH = 7.06. For example, the net initial hydrolysis rate in the pH 7.56 buffer at 30 °C was 8.4×10^{-8} mol L^{-1} s^{-1}, which was ~1.6 times the initial rate in the pH 7.06 buffer at the same temperature (5.1×10^{-8} mol L^{-1} s^{-1}). This is because the concentration of the nonprotonated MAPMA units of the block copolymer in the pH 7.56 buffer was higher than that in the 7.06 buffer. Calculations show that about 35% of the MAPMA units were in the nonprotonated state in the pH 7.56 buffer while 18% of the MAPMA units were nonprotonated in the pH 7.06 buffer.

For the reactions in both buffers, the plot of log V versus $1/T$ did not follow the Arrhenius equation in the entire studied temperature range but leveled off with the increase of temperature above a certain point, i.e., the reaction rate did not increase as much as anticipated from the Arrhenius equation. For the hydrolysis reactions in the pH 7.56 buffer, the transition temperature was ~39 °C, just above the CMT of the block copolymer in this buffer (37 °C), while the transition for the reactions in the pH 7.06 buffer occurred at ~42 °C, 2 °C above the CMT of the block copolymer in this buffer. Clearly, the thermo-induced micellization of PEO-*b*-P(DEGMMA-*co*-MAPMA) exerted an appreciable effect on the hydrolysis rate of NPA; the net initial rate was suppressed by the formation of micelles with the catalyst-containing block P(DEGMMA-*co*-MAPMA) forming the core in the aqueous buffers.

Since the pK_a of MAPMA units in the core of micelles could be different from that in water, we determined its value at 44 °C by the

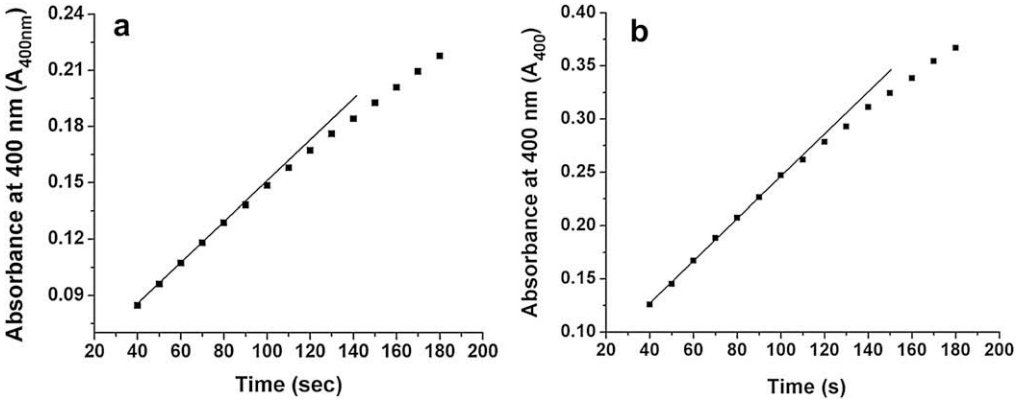

Fig. 6. Absorbance at 400 nm (A_{400}) recorded with a UV–vis spectrometer by a computer program as a function of time for the hydrolysis of *p*-nitrophenyl acetate using PEO-*b*-P(DEGMMA-*co*-MAPMA) as catalyst in the pH = 7.56 buffer at (a) 30 °C, which was below CMT, and (b) 44 °C, which was above CMT.

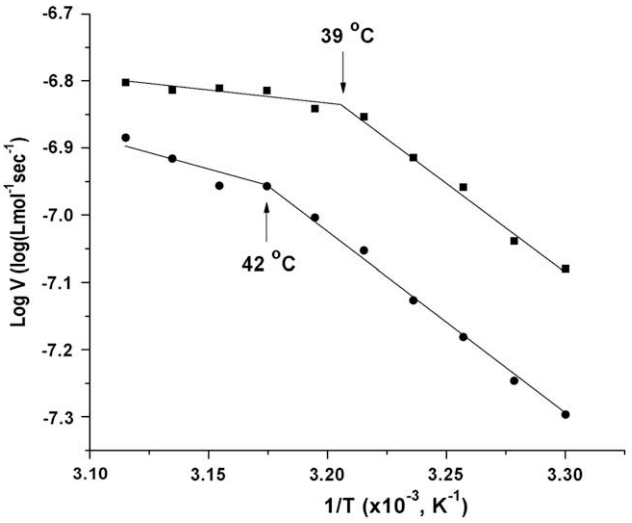

Fig. 7. Plot of the logarithm of net initial rate (log *V*) versus 1/*T* for the hydrolysis of *p*-nitrophenyl acetate catalyzed by PEO-*b*-P(DEGMMA-*co*-MAPMA) in the pH 7.56 buffer (■) and pH 7.06 aqueous buffer (●).

same method described in the Experimental section and found that it was 7.10, slightly lower than that at room temperature (7.91). Thus, the change of the pK_a before and after micellization cannot account for the suppression of the initial hydrolysis rate at temperatures above the CMT because a lower pK_a value means that the fraction of nonprotonated MAPMA units is higher, which should result in a higher reaction rate.

In our hydrolysis experiments, the polymer solution was equilibrated at each temperature for 25 min before the injection of the NPA solution. Thus, at temperatures above the CMT, micelles were already formed and the catalytic MAPMA units were buried inside the core of micelles. Therefore, the initial hydrolysis rate depends on how fast the reactants (NPA and water) can diffuse into the core of micelles. The study by Vaidya and Mathias has established that the first step in the hydrolysis mechanism is the rate-determining step (Scheme 3), which involves only NPA and DAAP, and the second step, the deacylation of acylpyridinium species in the presence of water, is the faster step [8]. In addition, there is a significant amount of water molecules associated with the thermosensitive block even at temperatures above the LCST. Thus, the initial hydrolysis rate or the rate of the formation of *p*-nitrophenoxide is dependent on the diffusion rate of NPA, not water molecules. NPA is an amphiphilic substrate with a partition coefficient of 7.4 between hexane and water (log $P = 0.87$ at 25 °C) according to the literature [24]. Our thermosensitive block is a polymethacrylate with an oligo(ethylene glycol) pendant from each repeat unit. Considering that its hydrophobicity is much lower than hexane even at temperatures above the LCST, we believe that the partition coefficient of NPA between the core of micelles and bulk water phase should be appreciably lower than 7.4. Thus, NPA is not strongly favored in the core of the micelles compared with the bulk water phase, i.e., the driving force for NPA molecules to diffuse into the core of micelles is not strong. On the other hand, DAAPs are known to be superior nucleophilic organic catalysts for the hydrolysis of activated esters [6–9]. Combining these two factors, it is very likely that the hydrolysis rate of NPA with PEO-*b*-P(DEGMMA-*co*-MAPMA) as catalyst at temperatures above the CMT is controlled by the diffusion rate of NPA from bulk water phase to the core of micelles. In other words, the reaction rate is determined by the mass transport limitation of NPA from bulk water phase to the core of micelles, which is imposed by the micellization of the block copolymer, resulting in the suppression of reaction rates compared with those predicted from the Arrhenius equation. Thus, the curve of log *V* versus 1/*T* leveled off with the increase of temperature.

From Fig. 7, one can also find that above the transition temperature the magnitude of the slope of the pH 7.56 curve is smaller than that of the pH 7.06 curve, i.e., the increase of reaction rate with temperature in the pH 7.56 buffer is more suppressed than that in the pH 7.06 buffer. This is likely because more MAPMA units of the block copolymer are protonated in the pH 7.06 buffer and thus are not active in the catalysis, causing the reaction rate to be more comparable to the diffusion rate of NPA than in the pH 7.56 buffer. In addition, the micelles might not be as tight as those in the pH 7.56 buffer because of more charged MAPMA units in the core; it could be slightly easier for NPA to diffuse into the core of micelles to access the buried catalytic sites.

4. Conclusions

A thermosensitive hydrophilic block copolymer with the thermosensitive block containing catalytic DAAP units, PEO-*b*-P(DEGMMA-*co*-MAPMA), was synthesized from macroinitiator PEO-Br by ATRP. The pK_a of the block copolymer at room temperature was 7.91, which was 1.40 pH units lower than that of EGMAP. DLS studies showed that the CMTs of PEO-*b*-P(DEGMMA-*co*-MAPMA) in the pH 7.06 and 7.56 buffers at a concentration of 0.020 wt% were 40 and 37 °C, respectively. Above 42 °C, well-defined micelles with the thermosensitive catalytic block forming the core were observed in both buffer solutions. The block copolymer was used as catalyst for the hydrolysis of NPA and the reactions were monitored by a UV–vis spectrometer. We found that the plot of logarithm of net initial hydrolysis rate versus inverse temperature did not follow the Arrhenius equation in the entire studied temperature range (30–48 °C), but leveled off with the increase of temperature above the CMT of the block copolymer in the buffer. Considering that NPA molecules must diffuse into the core of micelles and the DAAPs are superior nucleophilic organic catalysts for the hydrolysis of activated esters, the observed phenomenon is likely because the hydrolysis rate of NPA is controlled by the mass transport limitation of NPA from bulk water phase to the core of micelles. The block copolymer reported in this work represents a new type of stimuli-responsive polymer organocatalysts.

Acknowledgements

This work was supported by a grant from National Science Foundation (DMR-0605663).

References

[1] Benaglia M, Puglisi A, Cozzi F. Chem Rev 2003;103:3401–29.
[2] Bergbreiter DE. Chem Rev 2002;102:3345–83.
[3] Cozzi F. Adv Synth Catal 2006;348:1367–90.
[4] Overberger CG, Salamone JC. Acc Chem Res 1969;2:217–24.
[5] Overberger CG, Stpierre T, Vorchhei N, Lee J, Yaroslav S. J Am Chem Soc 1965;87:296–301.
[6] Hierl MA, Gamson EP, Klotz IM. J Am Chem Soc 1979;101:6020–1.
[7] Delaney EJ, Wood LE, Klotz IM. J Am Chem Soc 1982;104:799–807.
[8] Vaidya RA, Mathias LJ. J Am Chem Soc 1986;108:5514–20.
[9] Mathias LJ, Cei G. Macromolecules 1987;20:2645–50.
[10] Fife WK, Rubinsztajn S, Zeldin M. J Am Chem Soc 1991;113:8535–7.
[11] Rubinsztajn S, Zeldin M, Fife WK. Macromolecules 1991;24:2682–8.
[12] Wang GJ, Ye D, Fife WK. J Am Chem Soc 1996;118:12536–40.
[13] Bergbreiter DE, Osburn PL, Li CM. Org Lett 2002;4:737–40.
[14] Bergbreiter DE, Li CM. Org Lett 2003;5:2445–7.
[15] Deratani A, Darling GD, Fréchet JMJ. Polymer 1987;28:825–30.
[16] Deratani A, Darling GD, Horak D, Fréchet JMJ. Macromolecules 1987;20:767–72.
[17] Liang CO, Helms B, Hawker CJ, Fréchet JMJ. Chem Commun 2003;20:2524–5.
[18] Helms B, Liang CO, Hawker CJ, Fréchet JMJ. Macromolecules 2005;38:5411–5.

[19] Helms B, Guillaudeu SJ, Xie Y, McMurdo M, Hawker CJ, Fréchet JMJ. Angew Chem Int Ed 2005;44:6384–7.
[20] Tomoi M, Akada Y, Kakiuchi H. Makromol Chem Rapid Commun 1982;3:537–42.
[21] Menger FM, McCann DJ. J Org Chem 1985;50:3928–30.
[22] Huang JW, Shi M. Adv Synth Catal 2003;345:953–8.
[23] Wang GQ, Kuroda K, Enoki T, Grosberg A, Masamune S, Oya T, et al. Proc Natl Acad Sci U S A 2000;97:9861–4.
[24] Okhapkin IM, Bronstein LM, Makhaeva EE, Matveeva VG, Sulman EM, Sulman MG, et al. Macromolecules 2004;37:7879–83.
[25] Ge ZS, Xie D, Chen DY, Jiang X, Zhang Y, Liu H, et al. Macromolecules 2007;40:3538–46.
[26] Simmons MR, Patrickios CS. Macromolecules 1998;31:9075–7.
[27] Simmons MR, Patrickios CS. J Polym Sci Part A Polym Chem 1999;37:1501–12.
[28] Patrickios CS, Simmons MR. Colloids Surf A Physiochem Eng Aspects 2000;167:61–72.
[29] Scriven EFV. Chem Soc Rev 1983;12:129–61.
[30] Chen HT, Huh S, Wiench JW, Pruski M, Lin VSY. J Am Chem Soc 2005;127:13305–11.
[31] Zhao B, Jiang XM, Li DJ, Jiang XG, O'Lenick TG, Li B, et al. J Polym Sci Part A Polym Chem 2008;46:3438–46.
[32] Jiang XM, Wang BB, Li CY, Zhao B. J Polym Sci Part A Polym Chem 2009;47:2853–70.
[33] Han S, Hagiwara M, Ishizone T. Macromolecules 2003;36:8312–9.
[34] Aoshima S, Sugihara S. J Polym Sci Part A Polym Chem 2000;38:3962–5.
[35] Li DJ, Jones GL, Dunlap JR, Hua FJ, Zhao B. Langmuir 2006;22:3344–51.
[36] Li DJ, Zhao B. Langmuir 2007;23:2208–17.
[37] Zhao B, Li DJ, Hua FJ, Green DR. Macromolecules 2005;38:9509–17.
[38] Hua FJ, Jiang XG, Li DJ, Zhao B. J Polym Sci Part A Polym Chem 2006;44:2454–67.
[39] Hua FJ, Jiang XG, Zhao B. Macromolecules 2006;39:3476–9.
[40] Jiang XG, Zhao B. J Polym Sci Part A Polym Chem 2007;45:3707–21.
[41] Lutz JF, Weichenhan K, Akdemir O, Hoth A. Macromolecules 2007;40:2503–8.
[42] Li DJ, Dunlap JR, Zhao B. Langmuir 2008;24:5911–8.
[43] Matyjaszewski K, Miller PJ, Shukla N, Immaraporn B, Gelman A, Luokala BB, et al. Macromolecules 1999;32:8716–24.
[44] Miller PJ, Matyjaszewski K. Macromolecules 1999;32:8760–7.
[45] Zhao B, He T. Macromolecules 2003;36:8599–602.
[46] Jiang XG, Lavender CA, Woodcock JW, Zhao B. Macromolecules 2008;41:2632–43.
[47] Jiang XG, Zhao B. Macromolecules 2008;41:9366–75.
[48] Urry DW. J Phys Chem B 1997;101:11007–28.
[49] Rijcken CJF, Soga O, Hennink WE, van Nostrum CF. J Controlled Release 2007;120:131–48.
[50] Dimitrov I, Trzebicka B, Müller AHE, Dworak A, Tsvetanov CB. Prog Polym Sci 2007;32:1275–343.
[51] Gil ES, Hudson SM. Prog Polym Sci 2004;29:1173–222.